

A three-dimensional hybrid framework based on novel [Co₄Mo₄] bimetallic oxide clusters with 3,5-bis(3-pyridyl)-1,2,4-triazole ligands

Quan-Guo Zhai, Shu-Ni Li, Man-Cheng Hu* and Yu-Cheng Jiang

Key Laboratory of Macromolecular Science of Shaanxi Province, School of Chemistry and Materials Science, Shaanxi Normal University, Xi'an, Shaanxi 710062, People's Republic of China

Correspondence e-mail: hmch@snnu.edu.cn

Received 29 October 2008

Accepted 1 February 2009

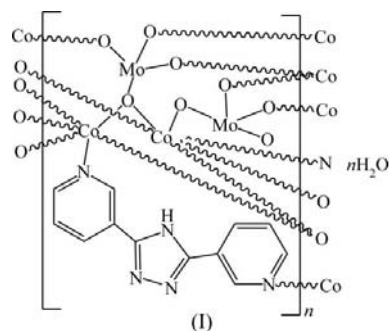
Online 13 February 2009

In the title organic–inorganic hybrid complex, poly[[[μ -3,5-bis(3-pyridyl)-1,2,4-triazole]tri- μ_3 -oxido-tetra- μ_2 -oxido-oxido-dicobalt(II)dimolybdenum(VI)] monohydrate], {[Co₂Mo₂O₈(C₁₂H₉N₅)·H₂O]_n}, the asymmetric unit is composed of two Co^{II} centers, two [Mo^{VI}O₄] tetrahedral units, one neutral 3,5-bis(3-pyridyl)-1,2,4-triazole (BPT) ligand and one solvent water molecule. The cobalt centers both exhibit octahedral [CoO₅N] coordination environments. Four Co^{II} and four Mo^{VI} centers are linked by μ_2 -oxide and/or μ_3 -oxide bridges to give an unprecedented bimetallic octanuclear [Co₄Mo₄O₂₂N₄] cluster, which can be regarded as the first example of a metal-substituted octamolybdate and exhibits a structure different from those of the eight octamolybdate isomers reported to date. The bimetallic oxide clusters are linked to each other through corner-sharing to give two-dimensional inorganic layers, which are further bridged by *trans*-BPT ligands to generate a three-dimensional organic–inorganic hybrid architecture with six-connected distorted α -Po topology.

Comment

The vast compositional range, considerable structural diversity, extensive physical properties and significant applications of inorganic oxides have stimulated continuous interest in the rational design of new metal oxides (Pope & Müller, 1991). In recent years, one powerful tool for the design of novel oxide solids has been the incorporation of organic molecules to alter the inorganic microstructure or to transmit structural preferences inherent in the coordination preferences of the metal centers (Stupp & Braun, 1997). Such organic–inorganic hybrid materials combine the unique characteristics of the components to provide novel structural types, as well as new prop-

erties arising from the synergistic interplay of the two components (Sanchez *et al.*, 2001, and references therein). Hargman *et al.* (1999) successfully exploited this method in the development of the structural chemistries of the molybdenum oxides of the Mo/O/M'/ligand family ($M' = \text{Fe, Co, Ni, Cu, Zn, etc.}$). Of this hybrid family, the most common example of a metal oxide is the octamolybdate anion [Mo₈O₂₆]⁴⁻, for which eight isomeric forms have been reported, namely $\alpha, \beta, \gamma, \delta, \epsilon, \zeta, \eta$ and θ . A comprehensive investigation of these isomers has been reported by Allis *et al.* (2004). However, to the best of our knowledge, no example of a transition-metal-substituted octamolybdate has been obtained to date. We report here the title complex, (I), in which an unprecedented bimetallic octanuclear [Co₄Mo₄O₂₂N₄] cluster is observed; this may be regarded as the first metal-substituted octamolybdate cluster and exhibits a structure different from any of the eight known isomers.



The title compound, (I), is composed of two-dimensional inorganic bimetallic layers based on unique [Mo₄Co₄] octanuclear clusters linked by 3,5-bis(3-pyridyl)-1,2,4-triazole (BPT) ligands to generate a three-dimensional organic–inorganic hybrid framework. As shown in Fig. 1, two independent [Mo^{VI}O₄] units, two Co^{II} cations, one neutral BPT ligand and one solvent water molecule occupy the asymmetric unit of (I). In the two [MoO₄] units, the Mo–O distances are in the range

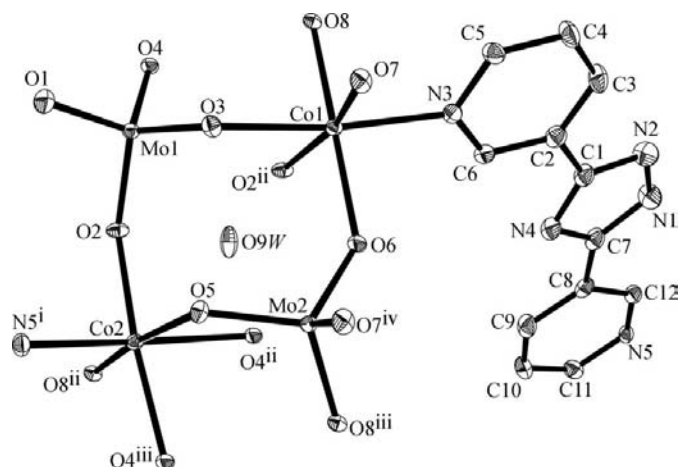


Figure 1

The asymmetric unit in (I), shown with 30% probability displacement ellipsoids. All H atoms have been omitted for clarity. [Symmetry codes: (i) $x, y, z + 1$; (ii) $-x + 1, -y + 1, -z + 1$; (iii) $x + 1, y, z$; (iv) $-x + 1, -y + 2, -z + 1$.]

1.699 (4)–1.818 (3) Å (Table 1). The coordination environments around Co1 and Co2 are both distorted octahedral, the six coordination sites being occupied by one N atom from a BPT ligand and five O atoms from five different [MoO₄] units. The Co–N distances are 2.129 (4) and 2.093 (4) Å, and the Co–O distances range from 2.051 (3) to 2.215 (3) Å. The corresponding bond angles around metal centers are in the ranges 106.57 (18)–112.61 (15)° for O–Mo–O, 80.54 (13)–99.43 (14)° and 163.80 (14)–170.73 (13)° for O–Co–O, and 86.20 (14)–102.10 (15)° and 171.84 (16)/173.08 (15)° for N–Co–O. Moreover, the Mo–O–Co angles range from 116.56 (16) to 164.8 (2)°.

Four [MoO₄] tetrahedra and four [CoNO₅] octahedra link to each other *via* corner- and edge-sharing to give an octanuclear [Co₄Mo₄O₂₂N₄] motif, as depicted in Fig. 2 (left). The structure can be described as a zigzag Co₄ cluster constructed from two pairs of [CoNO₅] octahedra linked through edge-sharing and capped on both faces by two [MoO₄] tetrahedra. Except for the four coordination sites occupied by the BPT N-atom donors, two Co1 octahedra and four capping [MoO₄] tetrahedra all contain two terminal oxide groups. Thus, there exist 12 μ_1 -O (where μ_1 -O denotes a terminal O atom), six μ_2 -O and four μ_3 -O atoms in this octanuclear cluster. This novel octanuclear motif can therefore be regarded as the first metal-

substituted octamolybdate cluster, although it is not a discrete structure. Comparison of the basic structural characteristics (Allis *et al.*, 2004) of the eight octamolybdate isomers reported to date indicates that the structure of [Mo₄Co₄O₂₂N₄] is unprecedented. It should be noted that although the δ -octamolybdate also consists of four octahedra and four tetrahedra, 14 μ_1 -O, ten μ_2 -O and two μ_3 -O atoms are observed. The empirical bond valence calculation for (I) led to calculated oxidation states of 5.856, 5.873, 2.121 and 2.173 for Mo1, Mo2, Co1 and Co2, respectively (Brown & Altermatt, 1985). The average values for the calculated oxidation states of molybdenum and cobalt are 5.865 and 2.147, which accord well with the charge neutrality of compound (I).

As depicted in Fig. 2 (right), ten terminal oxide groups from each octanuclear cluster act as μ_2 or μ_3 bridges linking four adjacent octanuclear motifs to generate a two-dimensional inorganic layer in the *ab* plane. Furthermore, all the BPT organic ligands adopt the *transoid* configuration (Dong *et al.*, 2005; Zhang *et al.*, 2005; Du *et al.*, 2008) and serve as μ_2 bridges, linking adjacent two-dimensional inorganic layers into a three-dimensional organic–inorganic hybrid framework (Fig. 3). For the purpose of classifying this three-dimensional hybrid structure, we define the [Mo₄Co₄] octanuclear cluster as a single point. Thus, the two-dimensional inorganic layer can be regarded as a four-connected 4⁴-net, and each octanuclear cluster links two adjacent [Mo₄Co₄] clusters from adjacent inorganic layers through four *trans*-BPT ligands. Each [Mo₄Co₄] motif can therefore be considered as a six-connected node with BPT molecules as linkers. The overall topology of this three-dimensional framework can be described as a distorted α -Po net because parallel inorganic (4,4)-nets are crosslinked by zigzag chains. The internode distances are 7.001 (1) and 9.332 (4) Å in the same inorganic (4,4)-net, and 14.646 (2) Å between two neighboring nets. It should be noted that of the currently known networks of α -Po topology, the majority are twofold or threefold interpenetrated frameworks (Wang *et al.*, 2006). However, (I) exhibits a non-interpenetrated structure owing to the existence of two-dimensional Mo–O–Co inorganic layers, in which the metal centers are only bridged by O atoms, which afford relatively short bridges. This linking mode generates an extraordinarily rigid two-dimensional net, which presents insufficient space for the interpenetration despite the linkage of the BPT organic ligands affording voids between adjacent inorganic layers.

Experimental

A mixture of Co(NO₃)₂·6H₂O (0.29 g, 1.0 mmol), Na₂MoO₄·2H₂O (0.12 g, 0.5 mmol), MoO₃ (0.07 g, 1.0 mmol) and 3,5-bis(3-pyridyl)-1,2,4-triazole (BPT) (0.22 g, 1.0 mmol) in water (10 ml) was introduced into a Parr Teflon-lined stainless steel vessel (25 ml), after which the vessel was sealed and heated at 453 K for 5 d under autogenous pressure. After the reaction had been cooled to room temperature over a period of 72 h, red crystals of (I) were produced (yield 51%, based on Mo). Analysis calculated for C₁₂H₁₁Co₂Mo₂N₅O₉: C 21.23, H 1.63, N 10.31%; found: C 21.35, H 1.58, N 10.33%.

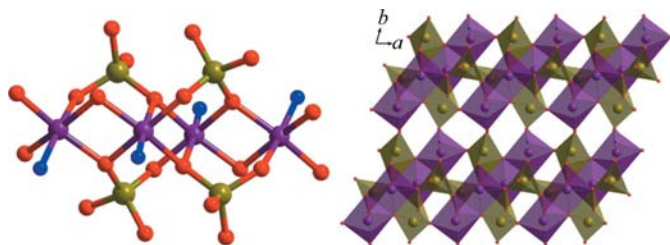


Figure 2
The unprecedented [Mo₄Co₄] octanuclear cluster (left) and a polyhedral representation of the two-dimensional inorganic layer (right) in (I).

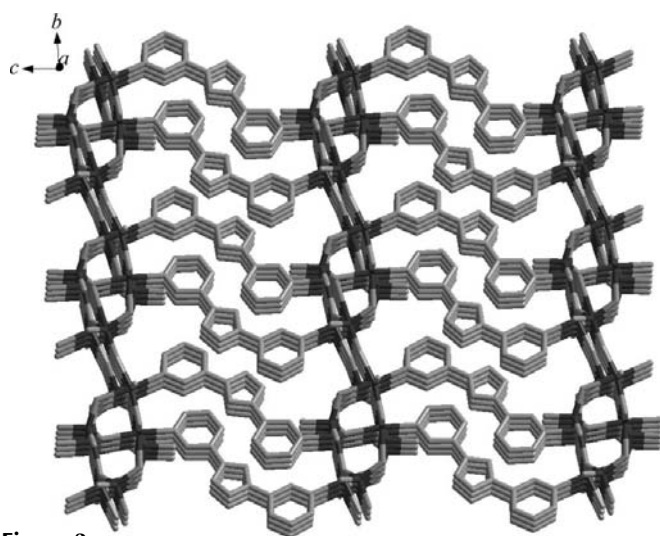


Figure 3
The three-dimensional organic–inorganic hybrid framework of (I), viewed along the *a*-axis direction. All H atoms have been omitted for clarity.

IR (KBr, cm^{-1}): 3438 (*w*), 1614 (*w*), 1411 (*w*), 921 (*m*), 869 (*m*), 786 (*m*), 647 (*s*), 549 (*w*).

Crystal data

[Co₂Mo₂O₈(C₁₂H₉N₅)]·H₂O
 $M_r = 679.00$
 Triclinic, $P\bar{1}$
 $a = 6.9999$ (3) Å
 $b = 9.3318$ (4) Å
 $c = 14.2802$ (12) Å
 $\alpha = 85.341$ (11)°
 $\beta = 84.805$ (11)°
 $\gamma = 75.127$ (9)°
 $V = 896.22$ (9) Å³
 $Z = 2$
 Mo $K\alpha$ radiation
 $\mu = 3.25$ mm⁻¹
 $T = 293$ (2) K
 $0.12 \times 0.10 \times 0.08$ mm

Data collection

Bruker SMART CCD diffractometer
 Absorption correction: multi-scan (SADABS; Sheldrick, 1996)
 $T_{\min} = 0.697$, $T_{\max} = 0.781$
 6929 measured reflections
 4027 independent reflections
 3434 reflections with $I > 2\sigma(I)$
 $R_{\text{int}} = 0.026$

Refinement

$R[F^2 > 2\sigma(F^2)] = 0.039$
 $wR(F^2) = 0.097$
 $S = 1.02$
 4027 reflections
 271 parameters
 H-atom parameters constrained
 $\Delta\rho_{\text{max}} = 1.35$ e Å⁻³
 $\Delta\rho_{\text{min}} = -1.05$ e Å⁻³

Table 1

Selected bond lengths (Å).

Mo1—O1	1.699 (4)	Co1—O8	2.117 (3)
Mo1—O3	1.753 (3)	Co1—N3	2.129 (4)
Mo1—O4	1.806 (3)	Co1—O3	2.138 (3)
Mo1—O2	1.818 (3)	Co1—O2 ⁱⁱⁱ	2.139 (3)
Mo2—O7 ⁱ	1.731 (3)	Co2—O5	2.051 (3)
Mo2—O5	1.755 (3)	Co2—O4 ⁱⁱ	2.073 (3)
Mo2—O6	1.770 (3)	Co2—O2	2.084 (3)
Mo2—O8 ⁱⁱ	1.808 (3)	Co2—O8 ⁱⁱⁱ	2.090 (3)
Co1—O6	2.054 (4)	Co2—N5 ^{iv}	2.093 (4)
Co1—O7	2.058 (4)	Co2—O4 ⁱⁱⁱ	2.215 (3)

Symmetry codes: (i) $-x + 1, -y + 2, -z + 1$; (ii) $x + 1, y, z$; (iii) $-x + 1, -y + 1, -z + 1$; (iv) $x, y, z + 1$.

The H atoms were positioned geometrically and included in the refinement using a riding model [C—H = 0.93 Å, N—H = 0.86 Å and O—H = 0.85 Å, and $U_{\text{iso}}(\text{H}) = 1.2U_{\text{eq}}(\text{parent atom})$]. The directions

of the O—H vectors were aligned with peaks initially located from difference maps. The maximum residual electron density of 1.35 e Å⁻³ is located 1.22 Å from atom O9W and the minimum density of -1.03 e Å⁻³ lies 0.82 Å from atom Mo2.

Data collection: SMART (Siemens, 1996); cell refinement: SAINT (Siemens, 1994); data reduction: SAINT; program(s) used to solve structure: SHELXS97 (Sheldrick, 2008); program(s) used to refine structure: SHELXL97 (Sheldrick, 2008); molecular graphics: SHELXTL (Sheldrick, 2008); software used to prepare material for publication: SHELXTL and publCIF (Westrip, 2009).

This paper is based on work supported by the National Natural Science Foundation of China (grant Nos. 20801033 and 20871079) and the Youth Foundation of Shaanxi Normal University.

Supplementary data for this paper are available from the IUCr electronic archives (Reference: BM3071). Services for accessing these data are described at the back of the journal.

References

- Allis, D. G., Rarig, R. S., Burkholder, E. & Zubieta, J. (2004). *J. Mol. Struct.* **688**, 11–31.
- Brown, I. D. & Altermatt, D. (1985). *Acta Cryst.* **B41**, 244–247.
- Dong, Y. B., Wang, H. Y., Ma, J. P., Huang, R. Q. & Smith, M. D. (2005). *Cryst. Growth Des.* **5**, 789–800.
- Du, M., Zhang, Z. H., You, Y. P. & Zhao, X. J. (2008). *CrystEngComm*, **10**, 306–321.
- Hagman, P. J., Hagman, D. & Zubieta, J. (1999). *Angew. Chem. Int. Ed.* **38**, 2638–2684.
- Pope, M. T. & Müller, A. (1991). *Angew. Chem. Int. Ed. Engl.* **30**, 34–48.
- Sanchez, C., Soler-Illia, G. J. de A. A., Ribot, F., Lalot, T., Mayer, C. R. & Calwil, V. (2001). *Chem. Mater.* **13**, 3061–3083.
- Sheldrick, G. M. (1996). SADABS. University of Göttingen, Germany.
- Sheldrick, G. M. (2008). *Acta Cryst.* **A64**, 112–122.
- Siemens (1994). SAINT. Siemens Analytical X-ray Instruments Inc., Madison, Wisconsin, USA.
- Siemens (1996). SMART. Siemens Analytical X-ray Instruments Inc., Madison, Wisconsin, USA.
- Stupp, S. I. & Braun, P. V. (1997). *Science*, **277**, 1242–1248.
- Wang, X. L., Qin, C., Wang, E. B. & Su, Z. M. (2006). *Chem. Eur. J.* **12**, 2680–2691.
- Westrip, S. (2009). publCIF. In preparation.
- Zhang, J. P., Lin, Y. Y., Huang, X. C. & Chen, X. M. (2005). *J. Am. Chem. Soc.* **127**, 5495–5506.